Learning about climate change uncertainty enables flexible water infrastructure planning

Sarah Fletcher

Institute for Data, Systems, and Society, Massachusetts Institute of Technology, Correspondence: sfletch@mit.edu

Megan Lickley

Department of Earth, Atmospheric, and Planetary Sciences, Massachusetts Institute of Technology

Kenneth Strzepek

Joint Program on the Science and Policy of Global Change, Massachusetts Institute of Technology

Note: This article is a non-peer reviewed preprint published at EarthArXiv

---

Abstract

Water resources planning requires making decisions about infrastructure development under substantial uncertainty in future regional climate conditions. However, uncertainty in climate change projections will evolve over the 100-year lifetime of a dam as new climate observations become available. Flexible strategies in which infrastructure is proactively designed to be changed in the future have the potential to meet water supply needs without over-building expensive infrastructure. Evaluating tradeoffs between flexible and traditional robust planning approaches requires extension of current scenario-based paradigms for water resources planning under climate uncertainty which take a static view of uncertainty. We develop a new dynamic planning framework that assesses the potential to learn about regional climate change over time and evaluates flexible approaches. We demonstrate it on a reservoir planning problem in Mombasa, Kenya. This approach identifies opportunities to reliably use flexible, incremental approaches, enabling climate adaptation investments to reach more vulnerable communities with fewer resources.

The challenge of infrastructure planning for climate change adaptation is exacerbated by uncertainty in climate projections [1]. Because of the large expense and widespread need for adaptation investments, planning models play a critical role in targeting available resources. Current approaches for water resources planning under climate uncertainty identify robust solutions that adequately meet performance goals across many potential climate scenarios [2, 3, 4, 5]. Flexible infrastructure planning has the potential to meet goals at reduced cost by building less infrastructure up front but designing options to expand in the future if needed [6, 7, 8, 9, 10]. Current planning models underestimate the potential of flexible infrastructure planning by taking a static view of uncertainty. Many long-term climate realizations are compared but not updated over time [11]. We develop a dynamic planning approach for water infrastructure planning under climate uncertainty. This approach appropriately evaluates flexible approaches by assessing 1) the potential to learn about climate change in the future and 2) the impacts of learning on investment decisions today.

Meeting performance goals like water reliability, cost, and access is a challenge for planners as water resource systems are stressed by climate change. Over the past 10 years, the planning research community has emphasized developing "robust" strategies that minimize regret by preparing for a wide range of possible future climates [12]. This has been important in developing adequate solutions that are relatively insensitive to our limited projections of climate change — even if they are suboptimal in any single climate realization. However, preparing for a wide range of climate scenarios leads to expensive overbuilding unless the worst outcomes are realized. Alternatively, planners can use a flexible approach in which plans are changed as uncertainties are realized over time. Flexibility in infrastructure planning and design is challenging yet important given the large capital costs and multidecadal lifetimes [13]. While flexible approaches may achieve reliability at reduced cost, they can also be more expensive by not taking advantage of economies of scale common in large infrastructure projects[14]. Additionally, short-term reliability outages can occur if infrastructure cannot be adapted quickly [15]. The impact of supply disruptions varies with end-use and setting. Appropriate methods are needed to weigh the risks and benefits of robust and flexible approaches given the natural, social, and technological context.

Water planning models typically assess infrastructure strategies statically by simulating many long-term climate realizations from GCMs and comparing the performance of each alternative strategy across simulations [16, 17]. GCM projections provide us with the best available estimates of how the global climate system will evolve under a given emissions scenario. However, as time passes and new climate observations are available, some GCM trajectories will prove to be more reliable than others. For example, suppose current projections estimate a range between 0.5 and 1.5 °C of change over the next 20 years. If after 20 years we observe 1.5 °C of change, this suggests the climate is warming in this region more rapidly than expected. We may now shift our projections of change upward for the following 20 years. Current approaches neglect this ability to learn about the accuracy of GCM projections over time [11, 18]. In reality, planners do take a dynamic approach, developing a new set of climate realizations when plans are revisited in 20 years that take into account how the climate has evolved in the interim. Planning models should reflect this, account for what we might learn in the future, and assess the impacts on planning decisions today.

We develop a dynamic planning framework, illustrated in Figure 1, that models the potential to learn about climate uncertainty over time and uses it to evaluate flexible planning strategies. We develop a set of "virtual climate observations" of mean temperature (T) and precipitation (P) that reflect the range of possible future climates indicated by current GCM projections. For each virtual climate observation, we use a Bayesian statistical model adapted from [19] to update climate uncertainty estimates. The updated estimates reflect what we will have learned if the virtual observation comes to pass. We use the updated uncertainty estimates to characterize the transition probabilities in a non-stationary stochastic dynamic program (SDP). This SDP planning formulation therefore takes into account all the potential new information that may be learned in the future. The SDP results develop optimal planning policies for each possible future climate in each time period. We use these polices to evaluate flexible infrastructure planning approaches and compare them to robust approaches. See Methods for details.

The UNEP estimates that the cost of climate change adaptation investments in the developing world may reach $500 billion per year by 2050 [20]. It is therefore essential to target infrastructure investments efficiently to reach the widest number of vulnerable communities. Flexible planning strategies are designed to react to changing conditions and information quickly without over investment. They are more likely to be promoted under a dynamic planning model that accounts for learning. To the authors' knowledge, this is the first framework that values the ability of flexible approaches to respond to

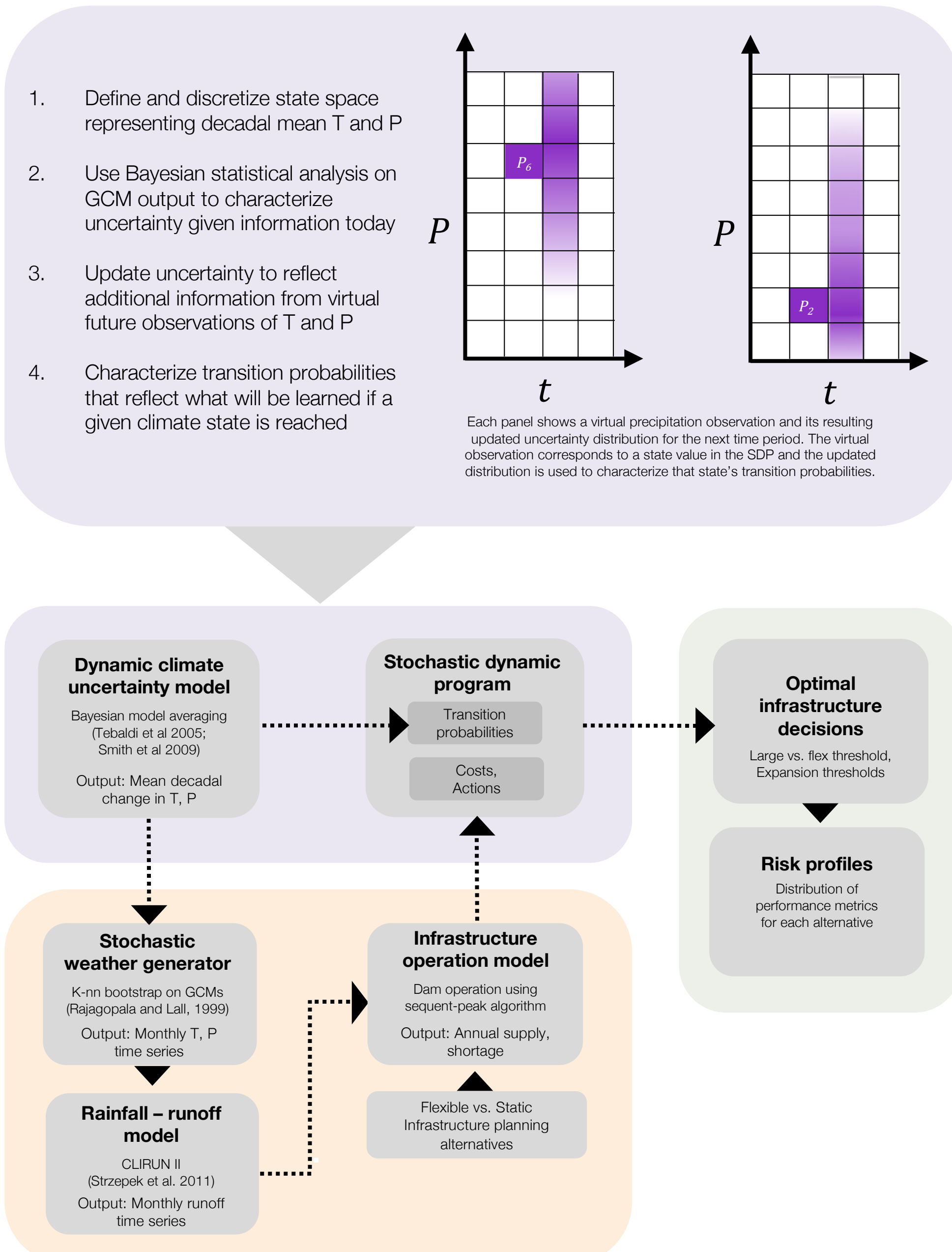

Figure 1: Schematic of integrated modeling framework.

learning, therefore more comprehensively evaluating the tradeoffs of robust and flexible adaptation strategies. This framework shows promise in identifying areas where smaller, flexible infrastructure is reliable, enabling billions of dollars of potential savings in climate change adaptation investments.

Results

We demonstrate this method with an application for Mombasa, Kenya. Mombasa is the second largest city in Kenya with an estimated population of 1.1 million [21]. Urban water demand is currently estimated at 150,000 m^3/day and expected to grow to 300,000 m^3/day by 2035 [22]. Mombasa has a warm, humid climate with average annual precipitation of 900 mm/yr and a mean annual temperature of 26°C [23]. Mean annual runoff (MAR) in the nearby Mwache river, the site of a proposed dam, is 113 MCM/yr [24].

Uncertainty in regional climate change projections makes it difficult to assess how large to size the dam in order to meet the yield and reliability targets over its full lifetime. While GCMs all project warming in the region, there is disagreement on the direction of precipitation change. This creates substantial uncertainty in changes in runoff and yield.

We apply our framework to develop and assess a flexible dam design. The flexible design enables extra storage capacity to be added if the initial dam becomes insufficient due to warmer, drier climates. We assess three planning scenarios, described in Table 1, intended to evaluate the sensitivity of our results to social and technological planning assumptions. In the low-demand scenarios, we assume a target yield of 150,000 m^3/day (54.8 MCM/yr) with 90% reliability from the Mwache dam. We evaluate the two dam sizes proposed by the previous World Bank study [18], 80 MCM and 120 MCM, as well as a flexible alternative in which the height of the smaller dam can be raised, increasing the reservoir capacity to 120 MCM. A high-demand scenario reflects future growth with a target yield of 300,000 cubic meters per day (m^3/d), greater than MAR and thus requiring the addition of a desalination plant; here we evaluate flexible desalination plant design in which additional capacity can be added.

Figure 2 a) and b) show historical observed T and P from the Climate Research Unit (CRU) [25] as well as individual GCMs' projected changes in

Table 1: Key planning scenarios and corresponding infrastructure evaluated. DR = discount rate; RO = reverse osmosis; Capex = capital expenditure.

Planning Scenario		Technology	DR	Capacity [MCM]		Capex [M$]			
				Small	Large	Small	Large	Exp	Flex + Exp
A	Low	Earthen dam	3%	80	120	76.5	99.2	49.6	148.8
B	Low	Earthen dam	0%	80	120	76.5	99.2	49.6	148.8
C	High	RO desalination	0%	60	80	183.1	232.2	72.4	255.5

T and P relative to 1990. 90% confidence interval (CI) of GCM projections are developed using our Bayesian uncertainty analysis and compared to CIs developed using a traditional democratic weighting. The Bayesian approach weights models based on how well they match historical observed changes in T and P (see Methods). The democratic approach assumes all models perform equally well [26]. Between these two methods, the Bayesian approach produces smaller CI because it assigns more weight to a subset of models that best match historical change.

A sample time series of virtual T and P observations and their corresponding updated uncertainty estimates are shown in Figure 2 c) and d). For each virtual observation, we simulate 10,000 virtual climate time series from the current observation to the end of the planning period and construct a 90% CI, shown by the shaded regions. This process is repeated for each time step, with darker colors in the plot corresponding to the CIs developed from virtual observations sampled later in the planning period. The darker CIs therefore reflect uncertainty estimates updated with information farther into the future.

Figure 2 e) and f) show how the simulated T and P observations update uncertainty in MAR and water shortages (assuming planning scenario A) respectively. While MAR correlates closely with precipitation, increased warming in the second half of the planning period offsets modest increases in P. Mean annual water shortages are measured against a 90% monthly reliability goal. Strong asymmetric uncertainty reflects the low-probability, high-severity risk of droughts; shortages occur only when runoff is substantially below MAR for several months.

An alternate time series of virtual time series and CIs analogous to panels c)-f) is shown in the SI. Across many different simulated T and P observa-

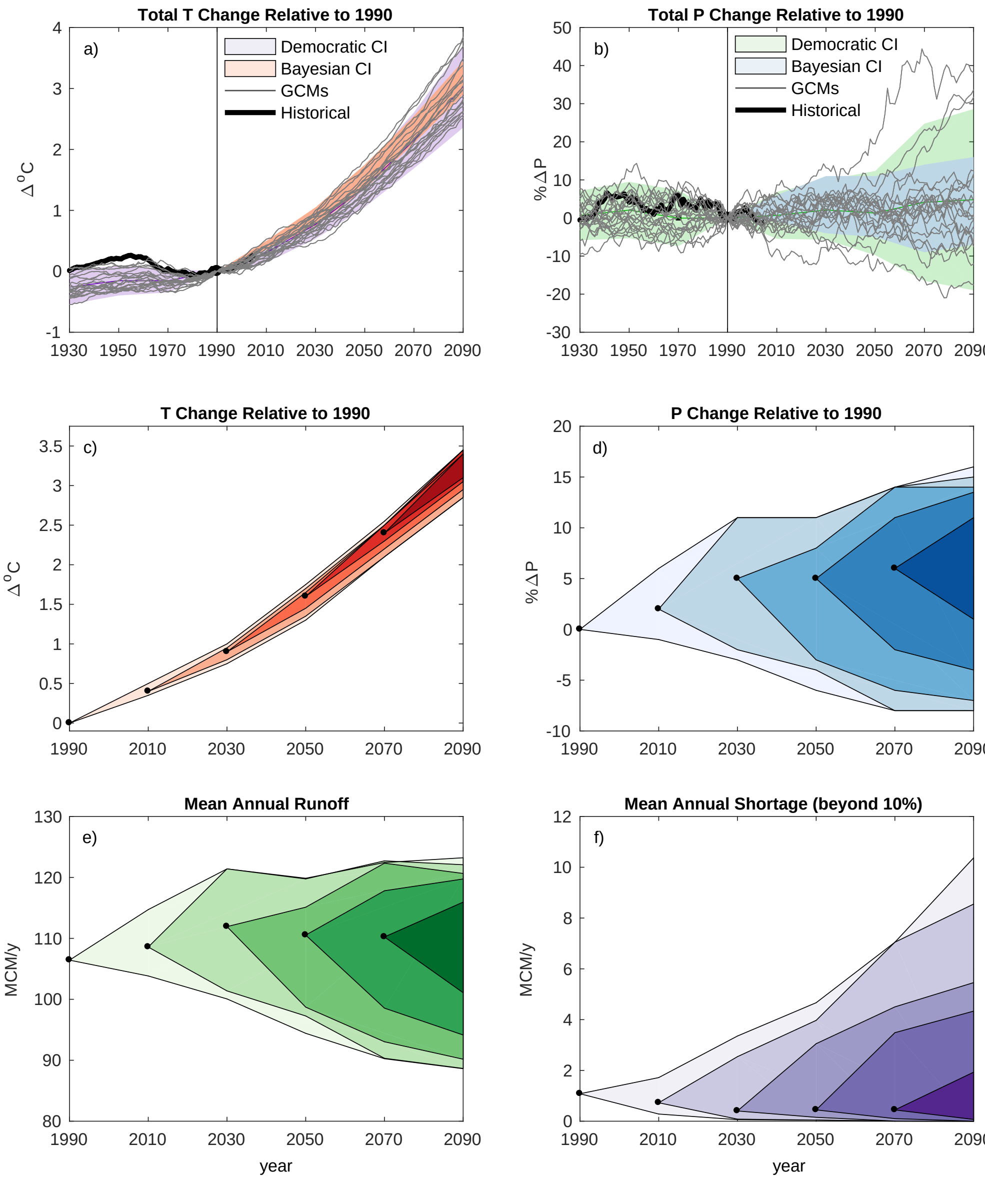

Figure 2: a)(or b)): Modeled and observed temperature (precipitation) relative to 1990 values with uncertainty estimates. Gray lines are 20-year moving averages of GCM simulations over Mombasa. Purple (green) shaded regions show the 90% CIs using the IPCC democratic weighting method,(i.e. $\pm 1.64 \times \sigma$). Orange (blue) shaded regions show the 90% CI developed using the Bayesian uncertainty method applied to historical observations before 1990. c)-f): One sample realization of Bayesian learning over time. Black dots represent a time series of virtual climate observations. Shaded regions indicate the projected 90% CI, updated with each time period's virtual observation. Virtual observations of T (c) and P (d) are used to simulate MAR (e), and water shortages (f).

tions we find a similar trend of narrowing of uncertainty in T, P, MAR and shortages, regardless of the direction of change, demonstrating a robust high value of information.

The simulated observations in the Bayesian analysis correspond to states in the SDP. The SDP optimal strategy accounts for all possible future observations and what would be learned if they were to be observed. In the first time period, shown in Figure 3 (a), the SDP develops a threshold as a function of T and P. Above the threshold, in hotter and drier climates, the robust dam is optimal and below it the flexible dam is. Due to the small cost difference between the flexible and large dam, investing in the robust (i.e. large dam) option upfront is preferred if the risk of shortages at the outset is high enough. This reduces expected costs by leveraging economies of scale. Panel b) shows expansion thresholds for time periods 2-5 for the flexible dam. Expanding infrastructure capacity is optimal in drier and warmer states. In the 2041-2060 time period, the policy threshold shifts right, reflecting the influence of learning and narrowing of uncertainty. In later time periods, however, it shifts left, reflecting the influence of the end of the planning horizon which disincentivizes investment.

Figure 4 shows infrastructure decisions under the optimal policy across 1000 simulated climate time series. In planning scenario A, the flexible alternative is chosen in 90% of simulations, shown in panel a). When the flexible alternative is chosen, the option to expand is never chosen in about 90% of simulations. This highlights the low probability of reaching a climate dry enough to generate shortages beyond 10% of demand. The time period at which expansion is exercised varies; more rapid warming and drying leads to earlier expansion. Panel b) shows cumulative distribution functions (CDFs) of the total cost (including shortage damages) of each alternative across the 1000 simulations under planning scenario A. The robust alternative has the same cost across simulations; as designed, no shortage damages are incurred in any feasible climate. The small dam performs better than the large dam in about 70% of simulations, but has substantially higher costs in 30% of simulations due to large damages from water shortages. The flexible dam mirrors the small dam in 70% of simulations, but the reliability risk is substantially mitigated because of the potential to expand. The high-end costs are higher than the robust alternative because 1) the cost of building the 80 MCM dam and expanding to 120 MCM is higher than building the 120 MCM dam upfront and 2) sometimes the dam is not expanded even when modest water shortages are incurred. The ability of the flexible alternative

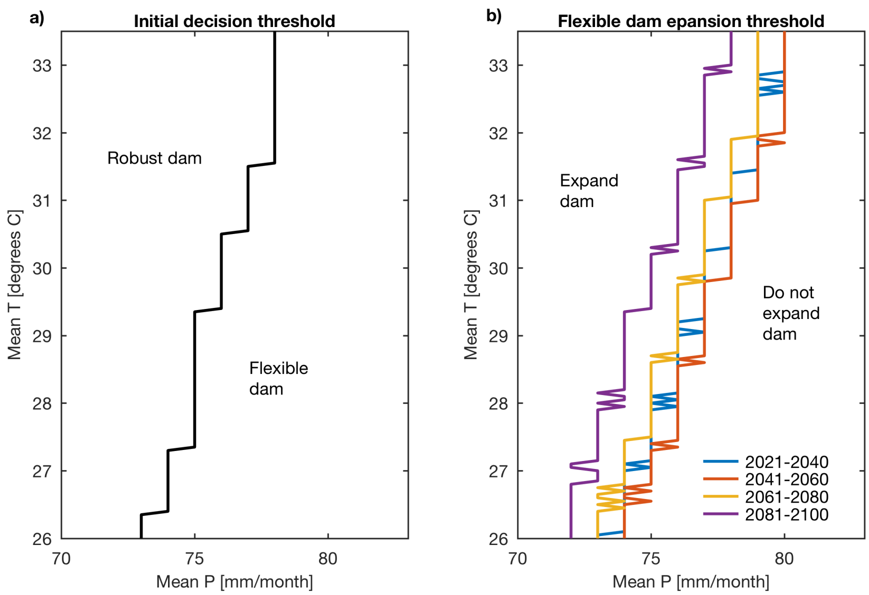

Figure 3: Optimal policies from SDP. a): Threshold for initial decision between robust and flexible design. b): Thresholds for exercising the option to increase height of flexible dam. Results shown for planning scenario A.

to mitigate both the the risk of overbuilding and the risk of severe shortages demonstrates the high value of flexibility in this case.

The value of flexibility changes under planning scenarios B (no discounting; panels c-d) and C (high demand with desalination plant; panels e-f). Without discounting, the robust dam is more favorable; it performs best in 60% of simulations, has no cost variability risk, and is chosen in 80% of simulations. Large economies of scale in the dam mean that a 120 MCM is only 30% more expensive than an 80 MCM dam for 50% additional capacity. This suggests it is often better to build the large dam upfront even if there is a relatively low probability that it will be needed.

Scenario C evaluates a 120 MCM dam combined with a desalination plant. We find a high value of flexibility even without discounting. The flexible alternative is chosen upfront in over 80% of forward simulations. The CDF demonstrates that it outperforms the static alternatives by substantially mitigating the over build risk in comparison to the robust alternative. The flexible alternative also modestly reduces the shortage damage risk in comparison to the small alternative. While the flexible alternative only reduces cost at the 90th percentile and above, this substantially reduces the expected value as the maximum cost of the small plant reaches almost M$400.

Looking across scenarios, the flexible alternative is chosen most often in scenario A because discounting incentivizes delayed capital investments. This is not the case in scenario B because large economies of scale incentivize a single, large investment. In scenario C more modest economies of scale lead to high value of flexibility in the absence of discounting, highlighting differences in the value of flexibility across technologies. Across all scenarios, the flexible dam is expanded in no more than 10% of simulations, highlighting the low probability of reaching a climate that is hot and dry enough to incur substantial shortages.

1. Discussion

The dynamic planning framework developed here accounts for the potential to learn about climate uncertainty in the future to assess the value of flexible infrastructure investments today. We develop an SDP in which virtual climate observations comprise the states. The SDP explicitly models learning about uncertainty through the use of non-stationary transition probabilities characterized by Bayesian climate uncertainty analysis. This approach captures the ability of flexibility to react to new information over

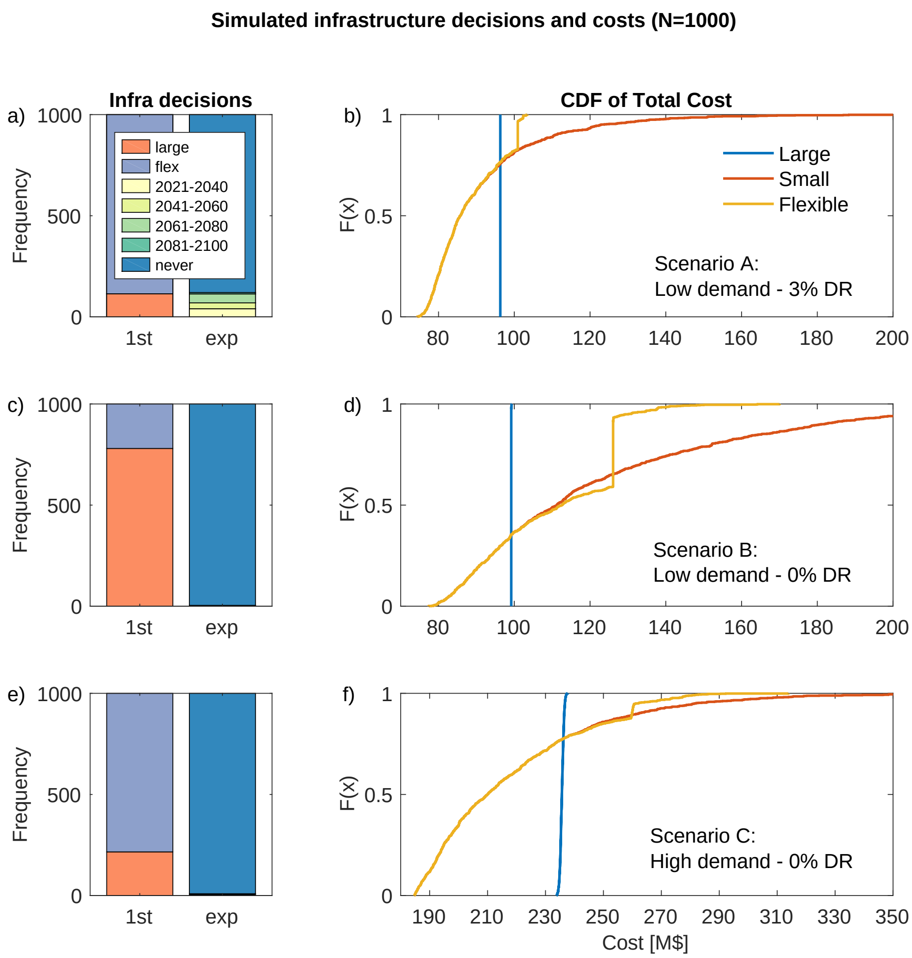

Figure 4: Simulated infrastructure decisions (left) and costs (right). a)-b): planning scenario A (low-demand, discounting). c)-d): planning scenario B (low-demand, no discounting); e)-f): planning scenario C (high-demand, no discounting.

time. We evaluate flexibility as an alternative planning strategy to achieve performance goals such as cost and reliability, rather than an end goal itself. This shows its ability to mitigate the risk of overbuilding in comparison to robust approaches while still preventing severe shortages.

The results in the Mombasa application demonstrate the nuances and tradeoffs inherent in comparing flexible and robust approaches for planning under climate uncertainty. Although the uncertainty and learning is driven by the climate system, decisions about whether flexibility is a valuable tool in mitigating risk are strongly influenced by social, technological, and economic factors. The large economies of scale in earthen dams make flexibility less valuable; it is better to choose a robust alternative when it is not much more expensive to do so. Reverse osmosis (RO) desalination, however, is an inherent modular technology with modest economies of scale, lending itself more readily to flexible planning. The discount rate, which trades off future adaptation goals for immediate rewards, promotes flexible approaches. Flexibility often delays investment, which can be especially impactful in resource-scarce areas where unused capital could support other critical infrastructure services. The value society places on access to reliable, sustainable water supplies — and the damage of short-term outages — is also influential. Future extensions to other planning problems which have differences in degree and nature of uncertainty, hydrological sensitivity to climate change, and social context can be used to assess under what conditions flexible, robust, and traditional planning approaches are more appropriate. Combining this learning approach with bottom-up vulnerability assessments that do not rely on probabilistic climate projections can address the limitations of GCM-based predictions. Identifying opportunities to learn and adapt flexibly can both enable efficient individual planning decisions as well as target collective climate change adaptation investments to reach a greater range of vulnerable communities.

[1] IPCC, Climate change 2013: the physical science basis. Contribution of working group I to the fifth assessment report of the intergovernmental panel on climate change., 2013.

[2] R. J. Lempert, D. G. Groves, Identifying and evaluating robust adaptive policy responses to climate change for water management agencies in the American west, Technological Forecasting and Social Change 77 (2010) 960–974.

[3] C. Brown, Y. Ghile, M. Laverty, K. Li, Decision scaling: Linking bottom-up vulnerability analysis with climate projections in the water sector, Water Resources Research 48 (2012) 1–12.

[4] J. R. Kasprzyk, P. M. Reed, G. W. Characklis, B. R. Kirsch, Many-objective de Novo water supply portfolio planning under deep uncertainty, Environmental Modelling and Software 34 (2012) 87–104.

[5] J. D. Herman, H. B. Zeff, P. M. Reed, G. W. Characklis, Beyond Optimality: Multistakeholder Robustness Tradeoffs for Regional Water Portfolio Planning Under Deep Uncertainty, Water Resources Research 50 (2014) 7692–7713.

[6] E. Z. Stakhiv, Pragmatic approaches for water management under climate change uncertainty, Journal of the American Water Resources Association 47 (2011) 1183–1196.

[7] European Comission, Adaptating infrastructure to climate change, Technical Report, Communication from the Commission to the European Parliament, the Council, The European Economic and Social Committee and the Committee of the Regions, 2013.

[8] M. Haasnoot, J. H. Kwakkel, W. E. Walker, J. ter Maat, Dynamic adaptive policy pathways: A method for crafting robust decisions for a deeply uncertain world, Global Environmental Change 23 (2013) 485–498.

[9] J. H. Kwakkel, M. Haasnoot, W. E. Walker, Developing dynamic adaptive policy pathways: a computer-assisted approach for developing adaptive strategies for a deeply uncertain world, Climatic Change 132 (2015) 373–386.

[10] H. B. Zeff, J. D. Herman, P. M. Reed, G. W. Characklis, Cooperative drought adaptation: Integrating infrastructure development, conservation, and water transfers into adaptive policy pathways, Water Resources Research 52 (2016) 7327–7346.

[11] W. E. Walker, M. Haasnoot, J. H. Kwakkel, Adapt or perish: A review of planning approaches for adaptation under deep uncertainty, Sustainability 5 (2013) 955–979.

[12] J. Herman, P. Reed, H. Zeff, G. Characklis, How Should Robustness Be Defined for Water Systems Planning under Change?, Journal of Water Resources Planning and Management 141 (2015) 4015012.

[13] O. L. de Weck, D. Roos, C. L. Magee, Engineering Systems: Meeting Human Needs in a Complex Technological World, MIT Press, Cambridge, MA, 2011.

[14] R. de Neufville, S. Scholtes, Flexibility in Engineering Design, MIT Press, Cambridge, Massachusetts, 2011.

[15] E. H. Y. Beh, H. R. Maier, G. C. Dandy, Adaptive, multiobjective optimal sequencing approach for urban water supply augmentation under deep uncertainty, Water Resources Research 51 (2015) 1529–1551.

[16] P. M. Reed, D. Hadka, J. D. Herman, J. R. Kasprzyk, J. B. Kollat, Evolutionary multiobjective optimization in water resources: The past, present, and future, Advances in Water Resources 51 (2013) 438–456.

[17] D. G. Groves, R. J. Lempert, A new analytic method for finding policy-relevant scenarios, Global Environmental Change 17 (2007) 73–85.

[18] World Bank Group, Enhancing the Climate Resilience of Africa's Infrastructure: The Power and Water Sectors, The World Bank, Washington, DC, 2015.

[19] R. L. Smith, C. Tebaldi, D. Nychka, L. O. Mearns, Bayesian Modeling of Uncertainty in Ensembles of Climate Models, Journal of the American Statistical Association 104 (2009) 97–116.

[20] United Nations Environment Programme, The Adaptation Finance Gap Report, Technical Report, Nairobi, Kenya, 2016.

[21] Central Intelligence Agency, The World Factbook: Kenya, `https://www.cia.gov/library/publications/the-world-factbook/geos/ke.html`, 2018.

[22] R. O. Ojwang, J. Dietrich, P. K. Anebagilu, M. Beyer, F. Rottensteiner, Rooftop rainwater harvesting for Mombasa: Scenario development with image classification and water resources simulation, Water (Switzerland) 9 (2017).

[23] M. New, M. Hulme, P. Jones, Representing twentieth-century space-time climate variability. Part II: Development of 1901-96 monthly grids of terrestrial surface climate, Journal of Climate 13 (2000) 2217–2238.

[24] CES Consultants, Feasibility Study, Preliminary and Detailed Engineering Designs of Development of Mwache Multi-Purpose Dam Project along Mwache River: Hydrology Report, Technical Report, Ministry of Regional Development, Nairobi, Kenya, 2013.

[25] I. Harris, P. D. Jones, T. Osborn, D. H. Lister, Updated high-resolution grids of monthly climatic observations–the cru ts3. 10 dataset, International journal of climatology 34 (2014) 623–642.

[26] R. Knutti, The end of model democracy?, Climatic Change 102 (2010) 395–404.

[27] The World Bank, World Bank Open Data, `https://data.worldbank.org/indicator/ER.GDP.FWTL.M3.KD?locations=SA`, 2010.

[28] E. Hawkins, R. Sutton, The potential to narrow uncertainty in projections of regional precipitation change, Climate Dynamics 37 (2011) 407–418.

[29] C. Tebaldi, R. L. Smith, D. Nychka, L. O. Mearns, Quantifying uncertainty in projections of regional climate change: A Bayesian approach to the analysis of multimodel ensembles, Journal of Climate 18 (2005) 1524–1540.

[30] K. E. Taylor, R. J. Stouffer, G. A. Meehl, An overview of CMIP5 and the experiment design, Bulletin of the American Meteorological Society 93 (2012) 485–498.

[31] J. Räisänen, T. N. Palmer, A probability and decision-model analysis of a multimodel ensemble of climate change simulations, Journal of Climate 14 (2001) 3212–3226.

[32] C. Miao, Q. Duan, Q. Sun, Y. Huang, D. Kong, T. Yang, A. Ye, Z. Di, W. Gong, Assessment of CMIP5 climate models and projected temperature changes over Northern Eurasia, Environmental Research Letters 9 (2014).

[33] J. Räisänen, How reliable are climate models?, Tellus, Series A: Dynamic Meteorology and Oceanography 59 (2007) 2–29.

[34] B. Boehlert, S. Solomon, K. M. Strzepek, Water under a changing and uncertain climate: Lessons from climate model ensembles, Journal of Climate 28 (2015) 9561–9582.

[35] C. Tebaldi, R. Knutti, The use of the multi-model ensemble in probabilistic climate projections, Philosophical Transactions of the Royal Society A: Mathematical, Physical and Engineering Sciences 365 (2007) 2053–2075.

[36] P. Block, B. Rajagopalan, Interannual Variability and Ensemble Forecast of Upper Blue Nile Basin Kiremt Season Precipitation, Journal of Hydrometeorology 8 (2007) 327–343.

[37] K. M. Strzepek, A. L. Mccluskey, Modeling the Impact of Climate Change on Global Hydrology and Water Availability, Technical Report, The World Bank, 2010.

[38] K. Strzepek, A. McCluskey, B. Boehlert, M. Jacobsen, C. Fant IV, Climate Variability and Change : A basin scale indicator approach to understanding the risk of climate variability and change: to water resources development and management, Technical Report, Word Bank, 2011.

[39] D. N. Yates, WatBal: An Integrated Water Balance Model for Climate Impact Assessment of River Basin Runoff, International Journal of Water Resources Development 12 (1996) 121–140.

[40] Z. Kaczmarek, Water balance model for climate impact analysis, Acta Geophysica Polonica 41 (1993) 423–437.

[41] Global Water Intelligence, Desal Data Cost Estimator, `https://www.desaldata.com/cost_estimator`, 2017.

Methods

The SDP uses Bayesian uncertainty analysis to develop a policy for 1) whether to invest in the flexible or robust alternative and, 2) if the flexible alternative is chosen, under what climate states and time periods it should be expanded. We develop forward simulations for different climate change paths by sampling from the transition probabilities to create time series of virtual climate observations. We use these virtual observation times series to assess the performance of the different alternatives when they operate according to the policies developed by the SDP. Probability distributions describe the performance against key performance metrics including cost and reliability. This approach follows that of engineering options analysis [14] as a tool for assessing the value of flexible engineering design. Each of the components of this analysis are detailed below.

Stochastic dynamic programming (SDP)

Stochastic dynamic programming is an optimization approach that represents decision-making under uncertainty using multiple stages or time periods. Optimal policies, representing the best possible action as a function of the system state and time period, are derived by recursively solving the Bellman equation (below).

$$V(s,t) = \underset{a \in A}{\operatorname{argmin}}\ C(s(t),a(t),t) + \gamma \sum_{s \in S} p(s(t{+}1) \,|\, s(t), a(t)) * V(t{+}1, s(t{+}1)) \tag{1}$$

where V is the optimal policy, t is the time period, a is an action, s is a state, γ is the discount rate, and $p(s(t+1) \,|\, s(t), a(t))$ are the transition probabilities. Here the state space S includes mean T and mean P averaged over a 20-year period. The action a describes whether a robust or flexible dam is chosen, and whether infrastructure capacity is expanded in later time periods. Costs C include the capital costs of infrastructure and damages if the infrastructure fails to meet reliability targets.

We formulate the Bellman equation as follows. The formulation is identical across planning scenarios A-C except where specified.

$$\begin{aligned} S &= \{T(t), P(t), Z(t)\} \\ A &= e(Z,t) \\ C &= I(T,P,Z,e,t) + D * U(T,P,Z,e,t) \end{aligned} \tag{2}$$

where

- $t \in \{1...5\}$ is a 20-year time period ranging from 2001-2020 for $t = 1$ to 2081-2100 for $t = 5$

- $T(t)$ is the mean temperature in °C in time period t, ranging from 25 to 33 at 0.05°C increments.

- $P(t)$ is the mean precipitation in mm/month in time period t, ranging from 66 to 97 at 1 mm/month increments.

- $Z(t) \in \{1...4\}$ is the available infrastructure, in which the states correspond to a small infrastructure alternative, large infrastructure alternative, flexible unexpanded alternative, and flexible expanded alternative, respectively. The infrastructure alternatives are either a set of dams (planning scenarios A and B) or a set of desalination plants (planning scenario C).

- $e(Z,t) \in \{0...4\}$ is the choice of infrastructure in which 0 is no change, 1 is a small alternative, 2 is a large/robust alternative, 3 is a flexible alternative, and 4 is the expansion of the flexible alternative. The alternatives include a set of dams (planning scenarios A and B) or a set of desalination plants (planning scenario C). The choices are constrained by time period and available infrastructure such that $e(Z,t=1) \in \{1,2,3\}\forall Z$; $e\{Z,t\} \in \{0,4\}\forall t = 2...5, Z = 3$; and $e\{Z,t\} \in \{0\}\forall t = 2...5, Z = 1,2,4$

- I is the cost of the infrastructure including capital costs (capex) and operating costs (opex). Desalination opex in planning scenario A is a function of the water produced in each time period.

- D is unit cost of damages incurred for unmet water demand, set at 15 \$ /m^3 in our base case based on estimates of water productivity in Kenya from the World Bank [27].

- U is the volume of unmet demand as a function of the climate states, existing infrastructure, and any new infrastructure brought online in time t. U=0 in t=1, reflecting that t=1 is a planning and construction period and performance is not measured until the beginning of the second 20-year time period.

Bayesian modeling of climate change uncertainty

We extend the Bayesian uncertainty analysis of [19] to characterize the SDP transition probabilities. We limit our focus to uncertainty in model structure rather than emissions or stochasticity 1) because structural uncertainty dominates long-term precipitation uncertainty [28] and 2) to utilize recent statistical methods for characterizing structural climate uncertainty [29, 19]. The approach in [19] uses ensembles of projections from the fifth phase of the Coupled Model Intercomparison Project (CMIP5) [30] to derive a single distribution describing uncertainty in climate change. In our approach, following [19], we use historical observations (or virtual historical observations) to estimate the reliability of each model run and therefore its weight in the resulting probability distribution. This is in contrast to the "democratic" approach used by [31] and Intergovernmental Panel on Climate Change (IPCC) in which each model projection is assumed equally likely and the multi-model mean and standard deviation is used to derive a single probability distribution.

We extend the Smith et al. (2009) statistical model in three ways. First, we apply the model to annually averaged P and T values separately, assuming that T and P are independent. This reflects that a model's performance in estimating T may be unrelated to its ability to estimate P. Second, we apply the model to observed and projected change in T and P (i.e.ΔT and $\%\Delta P$) rather than absolute T and P due to greater model skill in GCM projected changes in temperature and precipitation rather than absolute values [32, 33]. This is especially important in our application in Mombasa where there is less disagreement in temperature change than there is disagreement in hind-casted absolute temperature. Finally, we apply the model to multiple time periods in series. Smith et al. (2009) assumed two periods: a historical climate (1961-1990) and a future climate (2071-2100). We use pairs of 20-year time periods from 1980 to 2100, in which the "historical" climate corresponds to the time period in the SDP and the "future" climate corresponds to the next 20-year period; this provides the 1-stage transition probabilities needed in the SDP. The 20-year time interval was chosen so that interannual variability was not driving the trend in precipitation and temperature across time periods.

To implement the Bayesian uncertainty analysis in Mombasa, we use a total of 21 CMIP5 members whose modeling group and model run are included in SI Table 1. For each GCM, monthly temperature and precipitation values are averaged over 2°S to 6°S and 38°E to 42°E, overlaying the Mwache catchment; GCM projections are regridded from their original resolution following the approach in Boehlert (2015) [34]. The same is done for the observed climate, where monthly values are taken from the Climate Research

Unit (CRU) dataset version TS.3.21 [25]. The analysis is repeated for the five 20-year time periods starting with 2001-2020 for t=1 and ending with 2081-2100 corresponding to t=5 in the SDP.

Following [19], the statistical model is formulated as follows for ΔT; an identical and independent model is used for $\%\Delta P$.

$$\begin{aligned} X_0 &\sim N(\mu, \lambda_0^{-1}) \\ X_{j,t} &\sim N(\mu, \lambda_j^{-1}) \\ X_{j,t+1}|X_{j,t} &\sim N(\nu + \beta(X_j - \mu), (\theta\lambda_j)^{-1}), \end{aligned} \tag{3}$$

where X_0 is the observed ΔT in time period t, $X_{j,t}$ is model j's projection of ΔT in the current time period t, and $X_{j,t+1}$ is model j's projection of ΔT in the next time period $t+1$. X_0, $X_{j,t}$, and $X_{j,t+1}$ are treated as observations from unique normal distributions. μ and ν are the underlying means for the 20-year ΔT distributions in the current (t) and future $(t+1)$ time periods respectively. The goal of the analysis is to estimate a posterior distribution for ν, which will characterize the transition probabilities. λ_j is the inverse variance of X_j, representing the reliability of model j. β is a regression parameter that introduces correlation between $X_{j,t}$ and $X_{j,t+1}$; it is estimated by the model rather than assumed. θ is also an estimated parameter that enables a model to have different reliability in the future compared to the present. The marginal densities for each of the parameters are estimated using MCMC methods; we use the Gibbs sampling approach, parametric assumptions, and code developed in [19].

This approach does have limitations. First, it assumes that GCMs are independent of one another, when in fact some models borrow entire components from other models [35]. Second, we assume that a GCM's ability to reproduce ΔT or $\%\Delta P$ is a better indication of model performance than another metric, such as model variability. Additionally, we are simulating the potential to learn in the future using only models available today; repeating the analysis in 40 years with a broader range of models reflecting the new state of the science may produce larger shifts in CIs. However, this approach is the best available to assess learning in the future, which impacts planning decisions today. It enables a more precise, validated measure of uncertainty in comparison to the democratic approach used by the IPCC.

Stochastic weather generation

Climate impacts on river runoff depend on changes in month-to-month variability in precipitation and temperature in addition to changes in the mean. We model these two changes separately. To develop monthly timeseries of T and P, we follow the k nearest neighbors (kNN) approach as described in Rajagopalan et al., (1999) applied to GCM projections. This non-parametric statistical approach allows us to impose the mean T and P from the SDP while also capturing the standard deviation in monthly values and month-to-month autocorrelation projected by the GCMs. This approach was chosen for its simplicity and ease of implementation; future studies could use other non-parametric approaches such as the local polynomial regression method developed in [36]. For each 20-year time period, we employ the kNN approach to generate 100 samples of 20-year long monthly timeseries of T and P. The resulting time series are then applied to the Rainfall-runoff model presented below.

Rainfall-runoff model

Next, the synthetic T and P time series are input to a hydrological model to assess the impacts on runoff. We use CLIRUN II, the latest in a family of hydrological models developed to assess the impact of climate change on runoff [37, 38, 39, 40]. CLIRUN II is a two-layer, conceptual, lumped-watershed rainfall-runoff model. It averages soil parameters over the watershed and models runoff at one gauge station at the mouth of the basin. It can be run on a monthly or daily time step. Using the kNN generated samples of T and P, CLIRUN II generates a corresponding 100 samples of 20-year long monthly timeseries of runoff.

CLIRUN II is calibrated using 14 years of monthly streamflow data. Only one streamflow gauge, RGS 3MA03, is available in the Mwache basin [24]. However, it is directly upstream of the dam location, making it representative for this study. The same monthly temperature and precipitation data from CRU used in the Bayesian climate analysis is used to calibrate CLIRUN II for consistency. This temperature and precipitation data is different than the local data used in the previous World Bank study [18], leading to different calibration results but similar performance (historical MAR: 113 MCM/y; World Bank MAR: 133 MCM/y; our MAR: 103 MCM/y). Our analysis using CLIRUN II and the reservoir sizing model confirms that the 80 MCM dam meets the reliability targets in the current and expected future climate but does not meet reliability targets if the climate gets substantially warmer and drier. The 120 MCM dam meets reliability targets across all projected future climates, providing a robust alternative.

Infrastructure alternatives and operations

In planning scenarios A and B (current demand), capex and opex estimates for the small and robust dams were developed using the cost tool from the previous World Bank study [18]. For the flexible dam, the cost per m^3 of additional capacity added is assumed to be 50% greater than that of the original capacity.

In planning scenario C we assume a target yield of 300,000 m^3/d (109.6 MCM/y) with 90% reliability over the entire planning horizon, reflecting the potential for rapid demand growth on relatively short timescales. This high value of demand is consistent with 2035 projections from [22]. In this scenario, the target yield is greater than observed mean annual runoff in the Mwache river and therefore the dam cannot meet the target yield in today's climate regardless of its size. Therefore, we model the combination of a 120 MCM dam and a desalination plant that is used to supply demand when reservoir storage is low. Three desalination alternatives are chosen, analogous to the dam design alternatives. A low capacity alternative designed to meet reliability targets in the current and expected future climate with 60 MCM capacity; the robust alternative that meets the reliability targets across all projected future climates with 80 MCM capacity; a flexible alternative starts with 60 MCM and can be expanded to 80 MCM. Capex and opex estimates for the RO desalination plants were developed using the Cost Estimator tool from DesalData [41]. Evaluating this second scenario allows us to compare the value of flexibility across two technology options, earthen dams and desalination, which have unique water supply profiles and cost structures. These planning scenarios, and the cost and capacity of the infrastructure considered in each, is summarized in Table 1.

The infrastructure operation model includes dam operations (and desalination operations when necessary) that seek to meet the specified yield target while accounting for dead storage, net evaporation, and environmental flows. Unmet demand is measured for each of the 100 streamflow time series, and the average 20-year unmet demand is used to characterize U in the SDP formulation in equation 2.

Supplementary Information

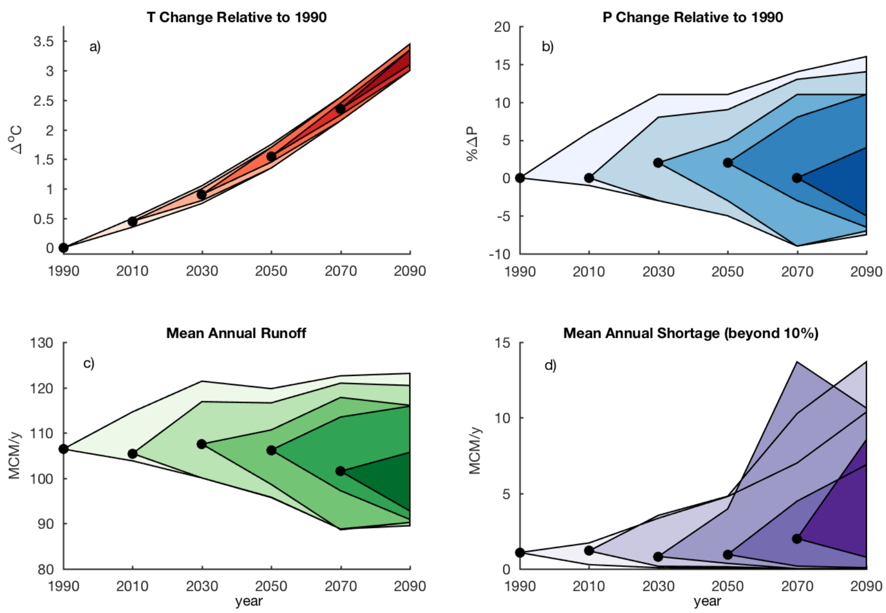

SI Figure 1: Alternate time series of virtual climate observation with corresponding learning in uncertainty estimates in T (panel a), P (panel b), MAR (panel c), and shortages beyond 10% assuming planning scenario A (panel d).

SI Table 1: Climate model ensembles used

Modeling Center	Institute ID	Model Name (ens. member)
Commonwealth Scientific and Industrial ResearchOrganization and Bureau of Meteorology, Australia	CSIRO/BOM	ACCESS 1.0 (1) ACCESS 1.3 (1)
Beijing Climate Center, China, Meteorological Administration	BCC	BCC-CSM1.1 (1)
EC-Earth Consortium	EC-EARTH	EC-EARTH (2, 8, 9, 12)
The First Institute of Oceanography, SOA, China	FIO	FIO-ESM (2, 3)
NOAA Geophysical Fluid Dynamics Laboratory	NOAA GFDL	GFDL-CM3 (1), GFDL-ESM2G (1), GFDL-ESM2M (1)
National Institute of Meteorological Research/Korea, Meteorological Administration	NIMR/KMA	HadGEM2-AO (1)
Met Office Hadley Centre	MOHC	HadGEM2-CC (1)
Japan Agency for Marine-Earth Science and Technology, Atmosphere and Ocean Research Institute (The University of Tokyo), and National Institute for Environmental Studies	MIROC	MIROC-ESM-CHEM (1) MIROC-ESM (1)
Atmosphere and Ocean Research Institute (The University of Tokyo), National Institute for Environmental Studies, and Japan Agency for Marine -Earth Science and Technology	MIROC	MIROC5 (1, 2, 3)
Norwegian Climate Centre	NCC	NorESM1-M (1), NorESM1-ME (1)